Supplementary Materials

Synthesis of SrFeO3-x/g-C3N4 heterojunction with improved visible-light photocatalytic activities in chloramphenicol and crystal violet degradation

Ho-Pan Lin [a], Chiing-Chang Chen [a]*, Wenlian William Lee [b,c]*, Ya-Yun Lai [d], Jau-Yuan Chen [a], Ya-Qian Chen [d], Jing-Ya Fu [a]

[a] Department of Science Application and Dissemination, National Taichung University of Education, Taichung 403, Taiwan

[b] Department of Occupational Safety and Health, Chung-Shan Medical University, Taichung 402, Taiwan

[c] Department of Occupational Medicine, Chung-Shan Medical University Hospital, Taichung 402, Taiwan

[d] Department of Applied Cosmetology, National Tainan Junior College of Nursing

* Author to whom correspondence should be addressed

E-mail: ccchen@ms3.ntcu.edu.tw; wllee01@csmu.edu.tw

Fax: +886-4-2218-3560

Tel: +886-4-2218-3406 ; +886-4-24730022

Table S1. Physical and chemical properties of as-prepared samples.

Photocatalysts	Specific surface area (m^2/g)	Pore volume (cm^3/g)	Pore diameter (nm)	Band gap (eV)
g-C_3N_4	17.60	0.1975	28.54	2.67
$SrFeO_{3-x}$	0.88	0.0055	33.01	--
1wt.%-500-2	20.54	0.2037	27.40	2.67
2wt.% -500-2	24.03	0.2305	26.50	2.67
4wt.% -500-2	40.89	0.3365	22.62	2.67
6wt.% -500-2	55.23	0.4187	22.19	2.67
8wt.% -500-2	65.62	0.4783	22.35	2.67
10wt.% -500-2	34.62	0.2816	23.10	2.67
30wt.% -500-2	33.99	0.1985	18.60	2.54
50wt.% -500-2	9.57	0.0619	20.90	--
70wt.% -500-2	4.31	0.0315	29.67	--
90wt.% -500-2	0.96	0.0145	54.77	--
4wt.% -400-2	11.38	0.1398	32.75	2.64
4wt.% -450-2	12.55	0.1432	31.07	2.66
4wt.% -500-2	40.89	0.3365	22.62	2.67
4wt.% -550-2	67.76	0.5264	25.90	2.66
4wt.% -600-2	N/A	N/A	N/A	--
4wt.% -500-1	19.39	0.1772	25.84	2.67
4wt.% -500-1.5	30.55	0.2316	21.10	2.67
4wt.% -500-2	40.89	0.3365	22.62	2.67
4wt.% -500-2.5	45.73	0.2986	18.32	2.67
4wt.%-500-3	64.26	0.4287	19.13	2.67

Table S2. Structure of photodecomposed products in the CAP photodegradation process by g-C_3N_4/$SrFeO_{3-x}$.

Peak no.	Compound Structure	Peak no.	Compound Structure
1	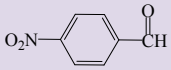	8	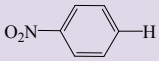
2	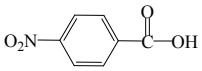	9	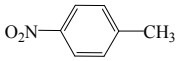
3	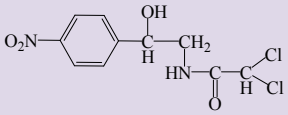	10	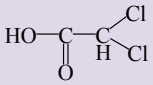
4	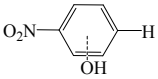	11	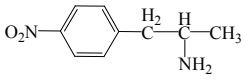
5(CAP)	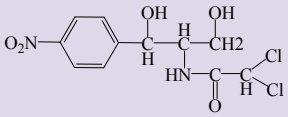	12	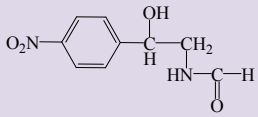
6	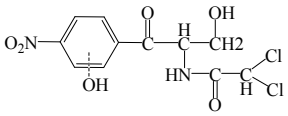	13	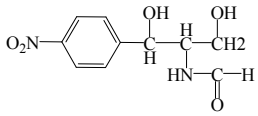
7	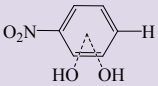		

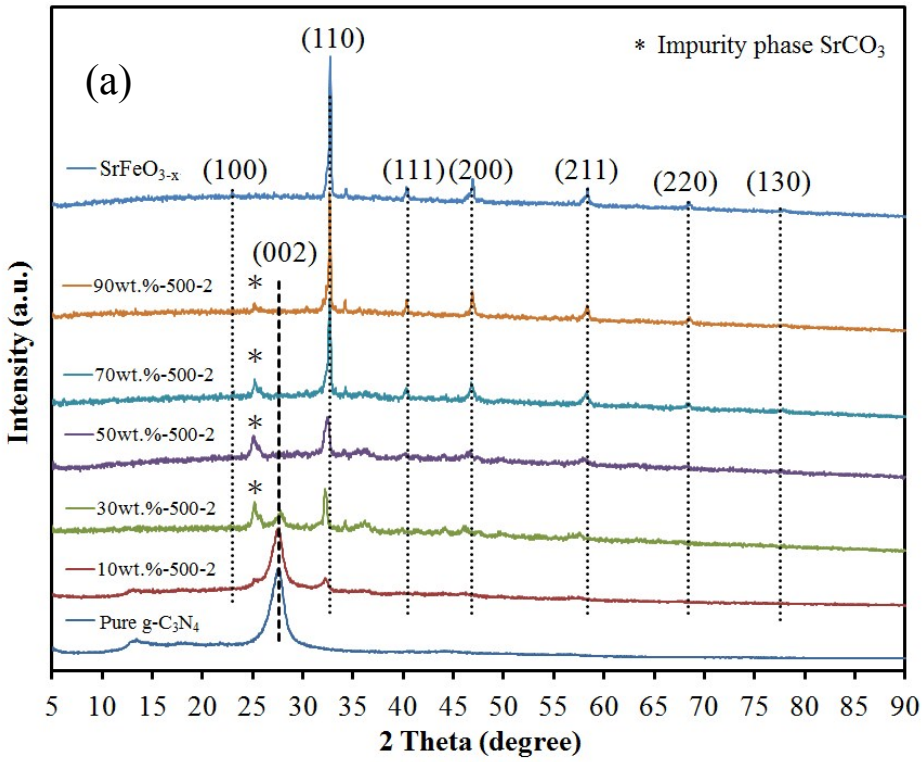

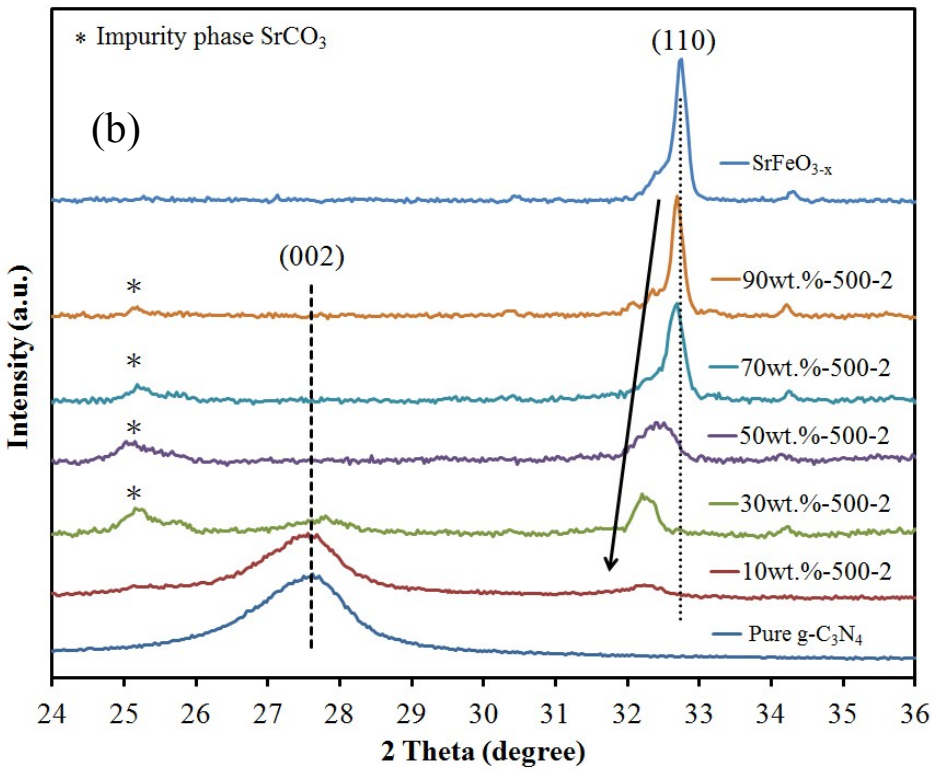

Figure S1. (a) XRD patterns of as-prepared samples under different weight percentage. (b) enlarged view. (Reaction conditions: sintering temp = 500°C, time = 2 h)

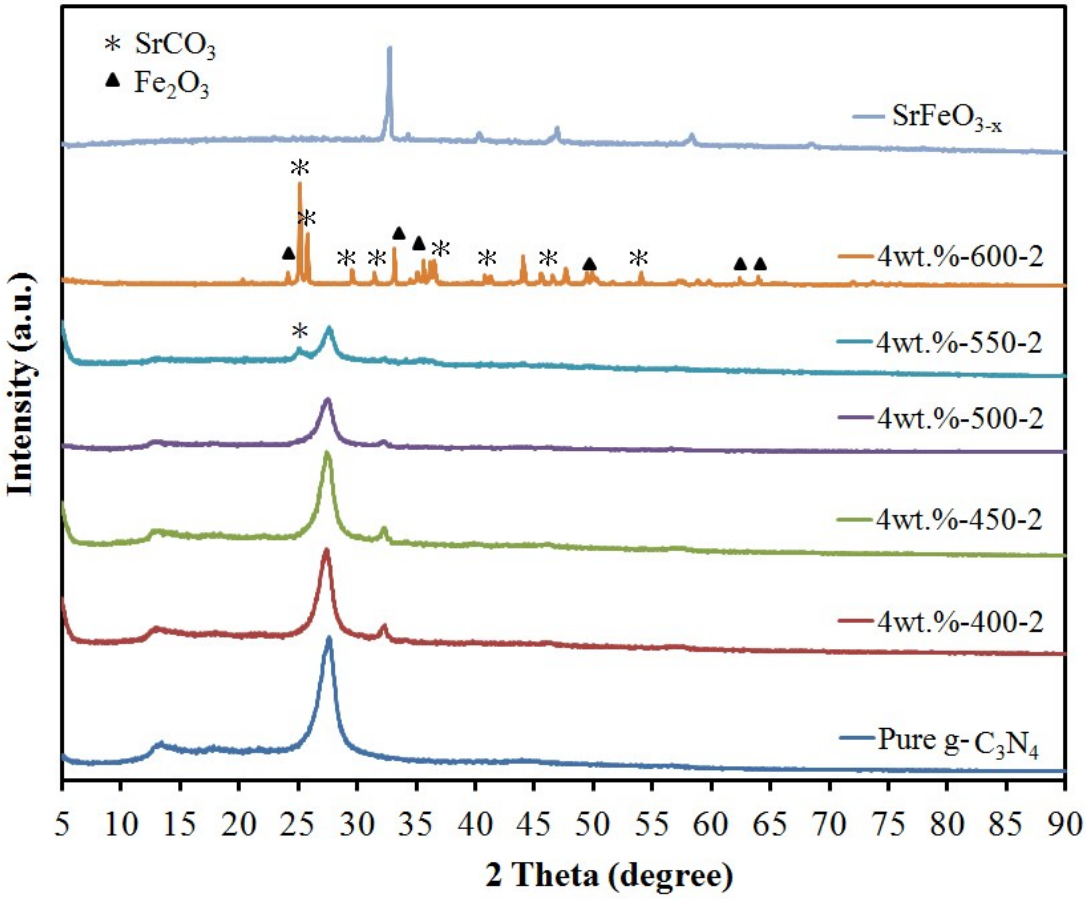

Figure S2. XRD patterns of as-prepared samples under different sintering temperature. (Reaction conditions: 4wt%, time = 2 h)

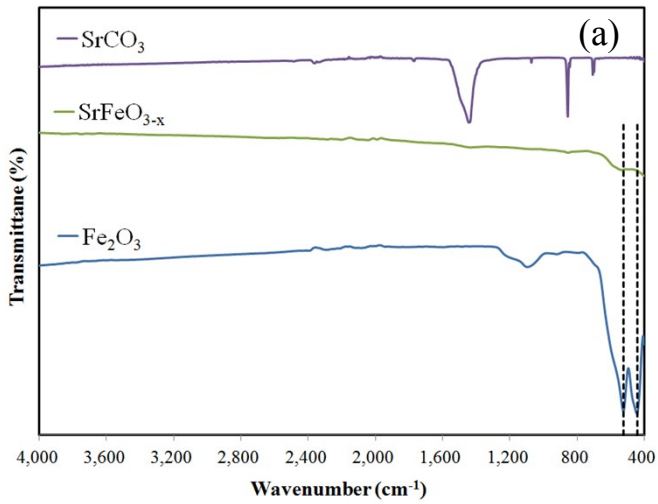

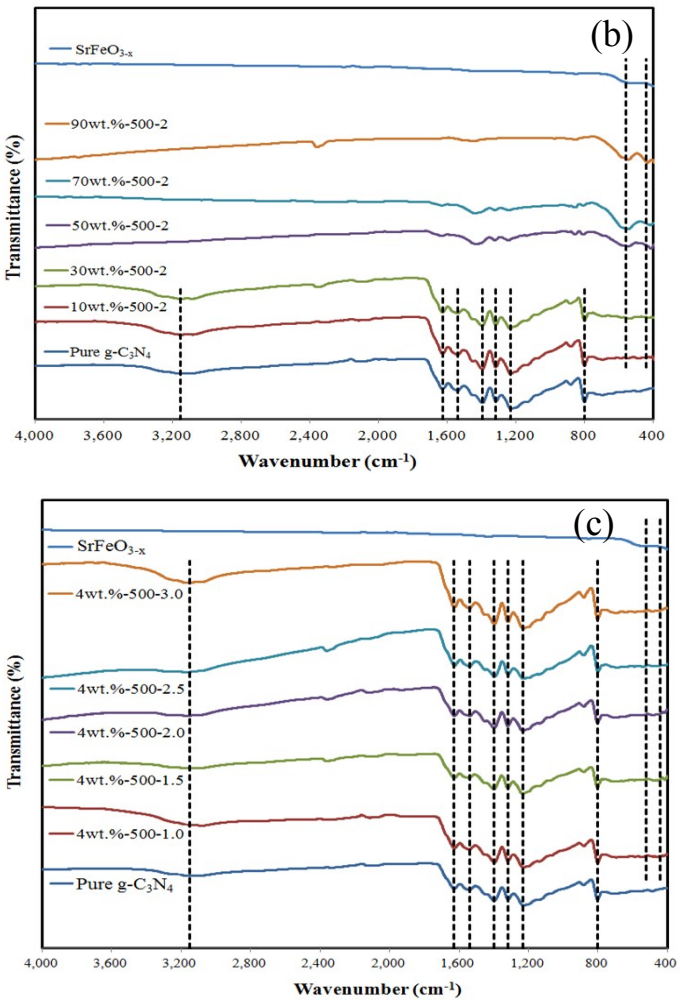

Figure S3. XRD patterns of (a) $SrCO_3$, $SrFeO_{3-x}$,and Fe_2O_3, as-prepared samples (b) under different weight percentage (reaction conditions: sintering temp = 500°C, time = 2 h), (c) under different teaction time (reaction conditions: sintering temp = 500°C, 4wt.%).

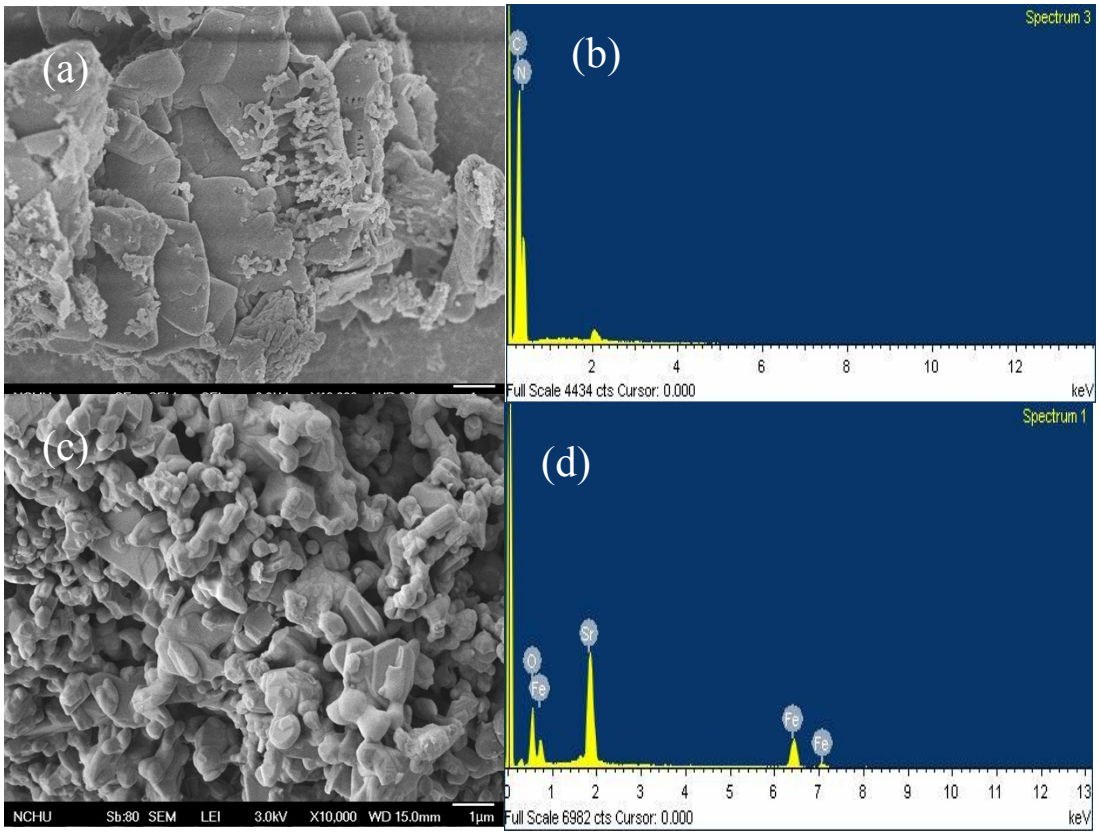

Figure S4. SEM images and EDS of (a) (b) $SrFeO_{3-x}$ and (b) (c) g-C_3N_4.

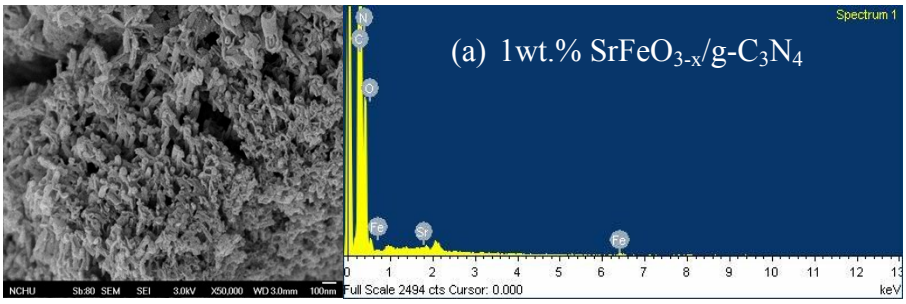
(a) 1wt.% $SrFeO_{3-x}/g-C_3N_4$
Spectrum 1
Full Scale 2494 cts Cursor: 0.000
keV

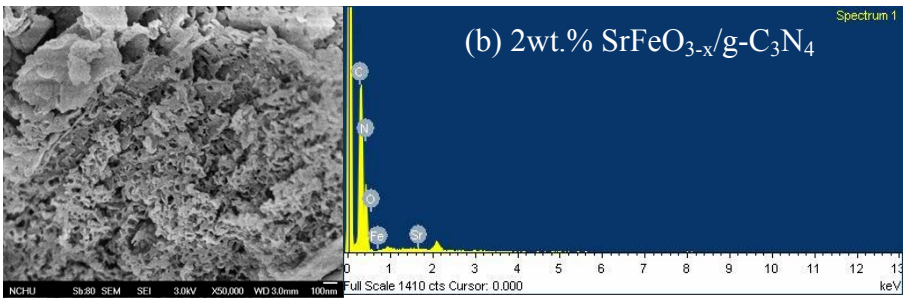
(b) 2wt.% $SrFeO_{3-x}/g-C_3N_4$
Spectrum 1
Full Scale 1410 cts Cursor: 0.000
keV

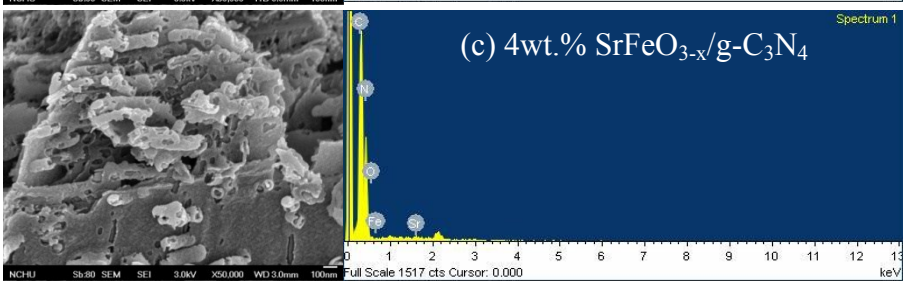
(c) 4wt.% $SrFeO_{3-x}/g-C_3N_4$
Spectrum 1
Full Scale 1517 cts Cursor: 0.000
keV

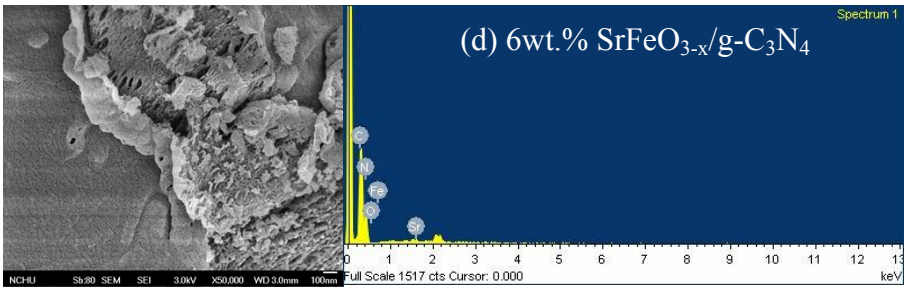
(d) 6wt.% $SrFeO_{3-x}/g-C_3N_4$
Spectrum 1
Full Scale 1517 cts Cursor: 0.000
keV

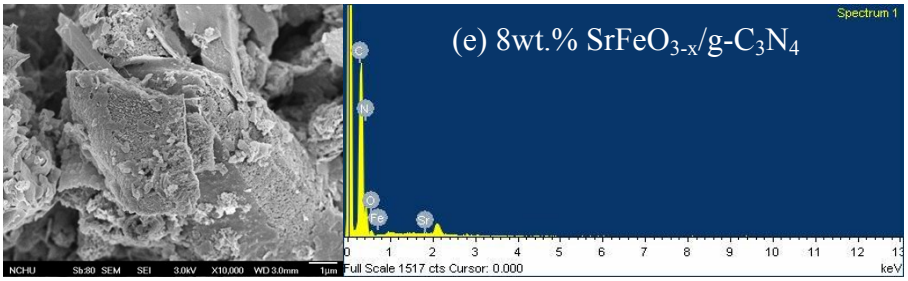
(e) 8wt.% $SrFeO_{3-x}/g-C_3N_4$
Spectrum 1
Full Scale 1517 cts Cursor: 0.000
keV

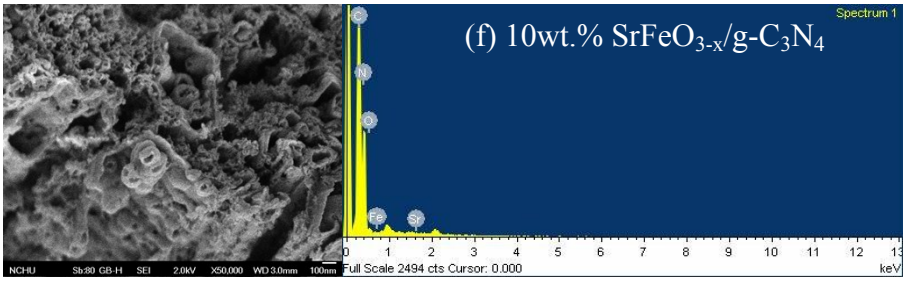
(f) 10wt.% $SrFeO_{3-x}/g-C_3N_4$
Spectrum 1
Full Scale 2494 cts Cursor: 0.000
keV

Figure S5. SEM images and EDS of $SrFeO_{3-x}$/g-C_3N_4 prepared by the sintering method at different weight percentage with $SrFeO_{3-x}$. (Sintering conditions: temp = 500°C, time = 2 h)

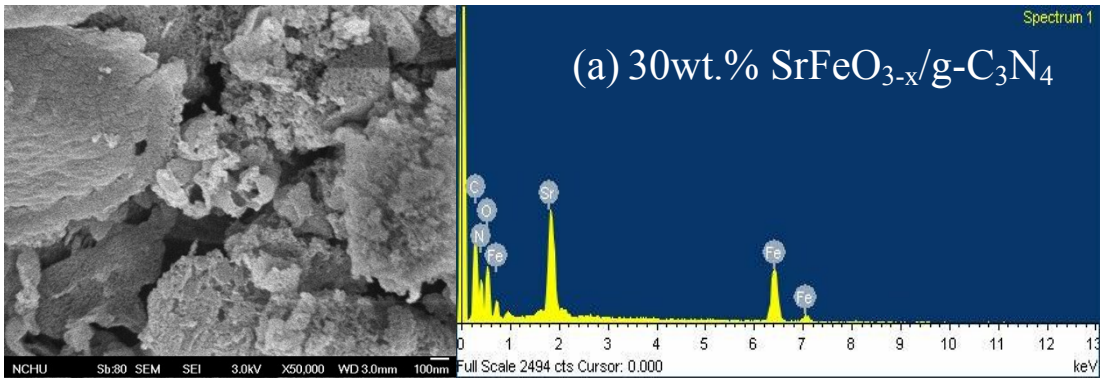

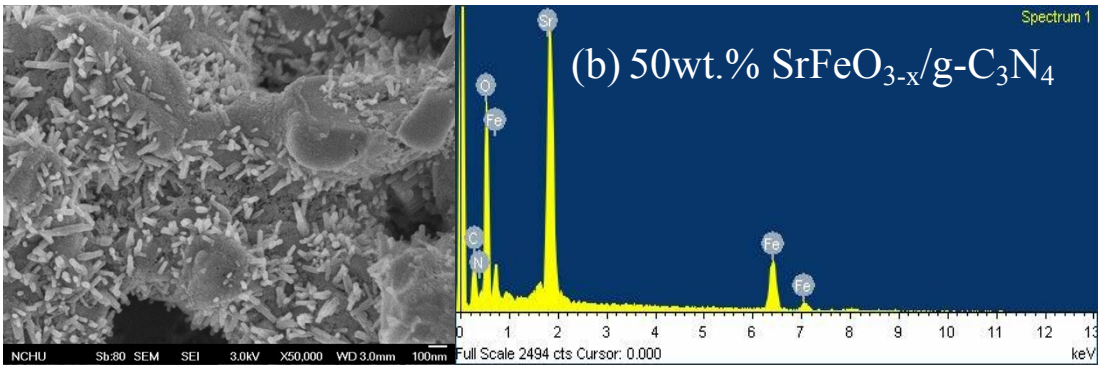

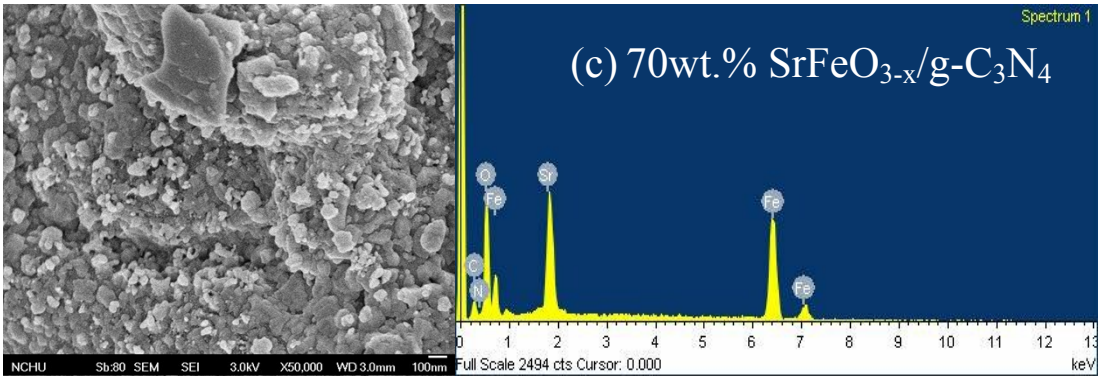

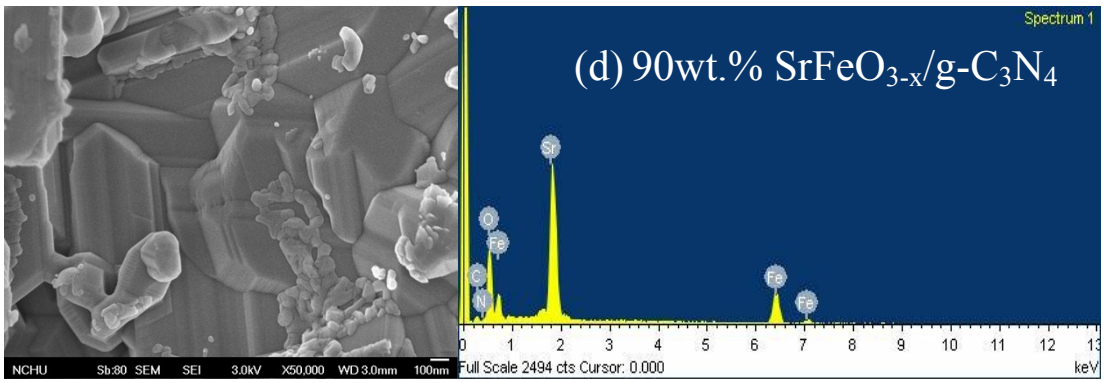

Figure S6. SEM images and EDS of $SrFeO_{3-x}$/g-C_3N_4 prepared by the sintering method at different weight percentage with $SrFeO_{3-x}$. (Sintering conditions: temp = 500°C, time = 2 h)

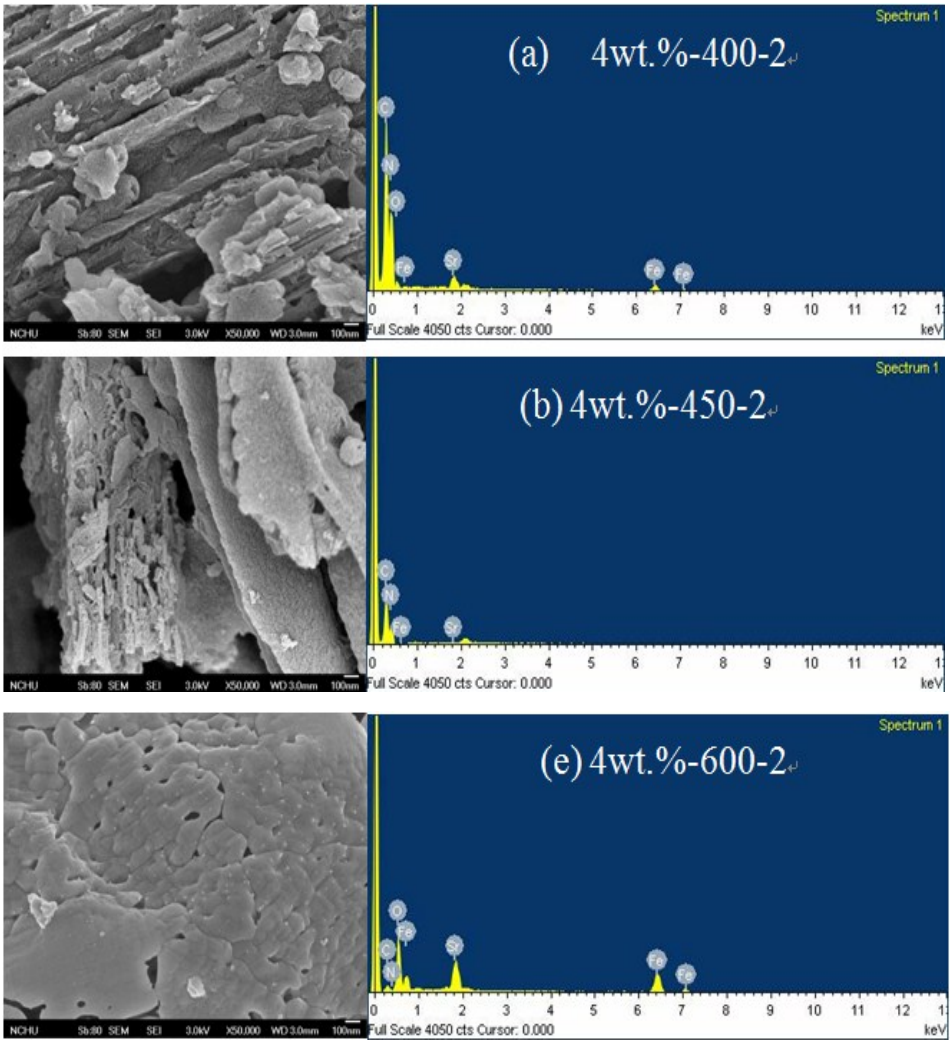

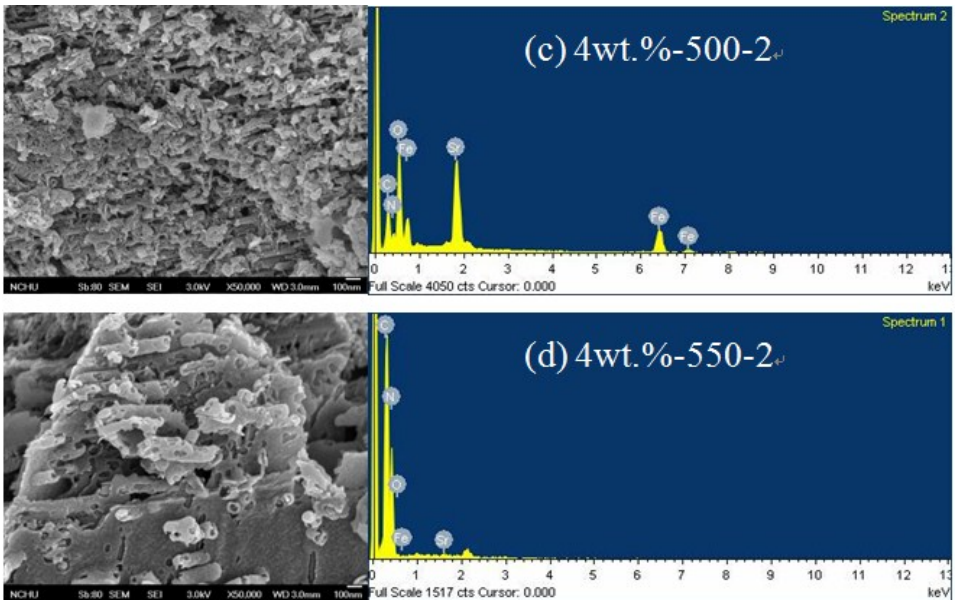

Figure S7. SEM images and EDS of $SrFeO_{3-x}$/g-C_3N_4 prepared by the sintering method at different temperature. (Sintering conditions: 4 weight percentage $SrFeO_{3-x}$, time = 2 h).

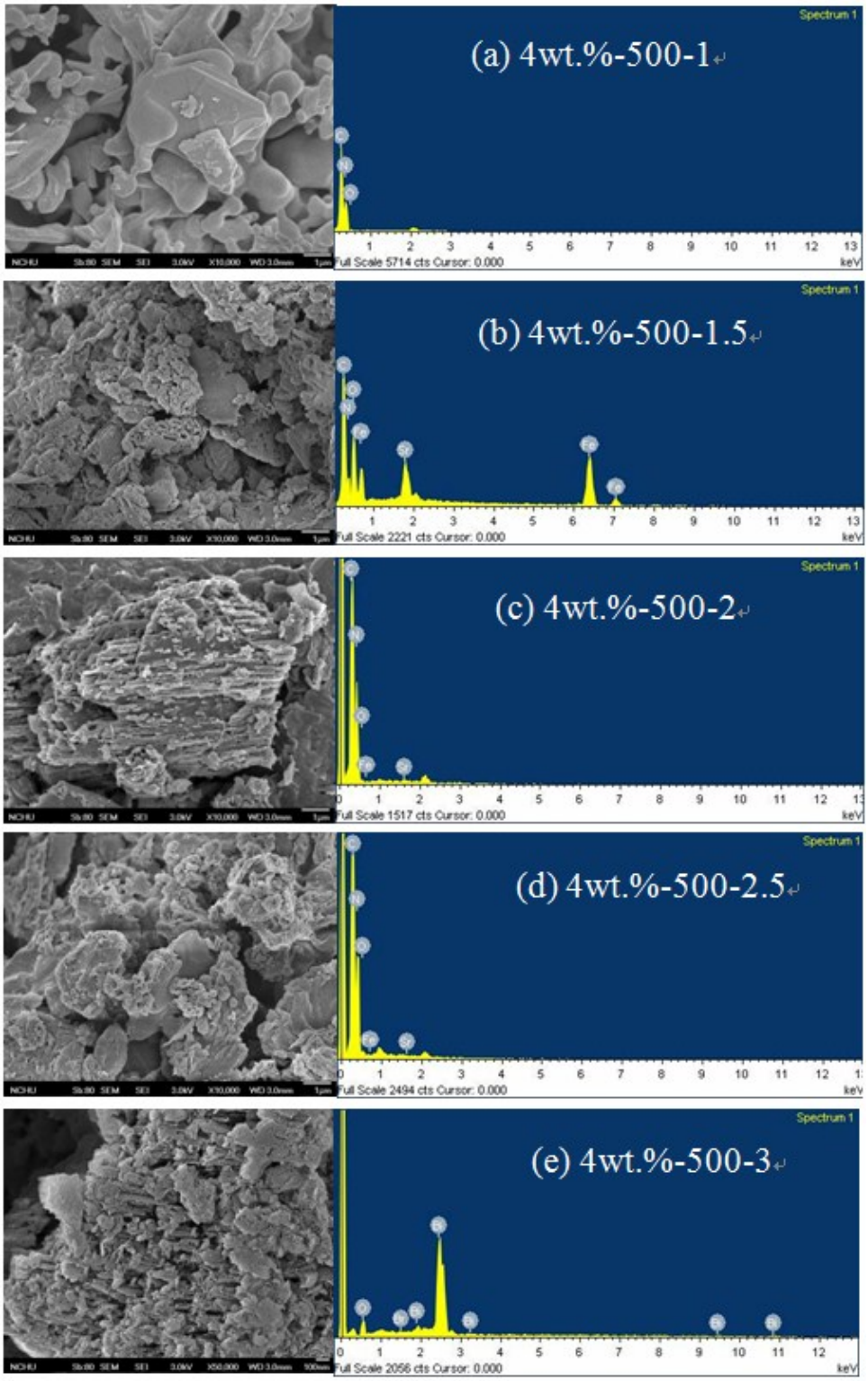

Figure S8. SEM images and EDS of $SrFeO_{3-x}$/g-C_3N_4 prepared by the sintering method at different time. (Sintering conditions: 4 weight percentage $SrFeO_{3-x}$, temp = 500°C).

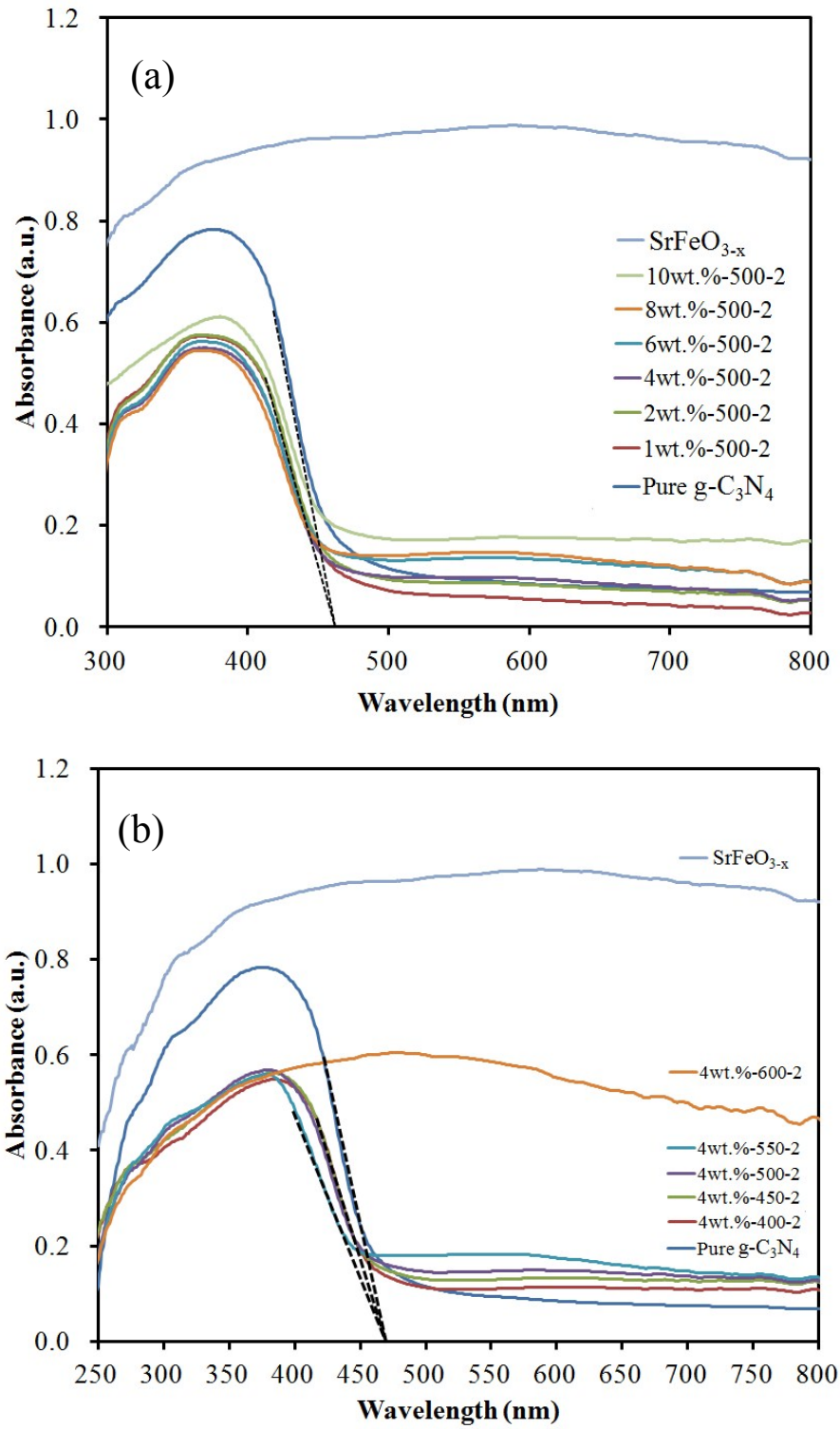

Figure S9. UV-vis diffuse reflectance spectra of the $SrFeO_{3-x}$/g-C_3N_4 samples: (a) weight percentage and (b) reaction temperature.

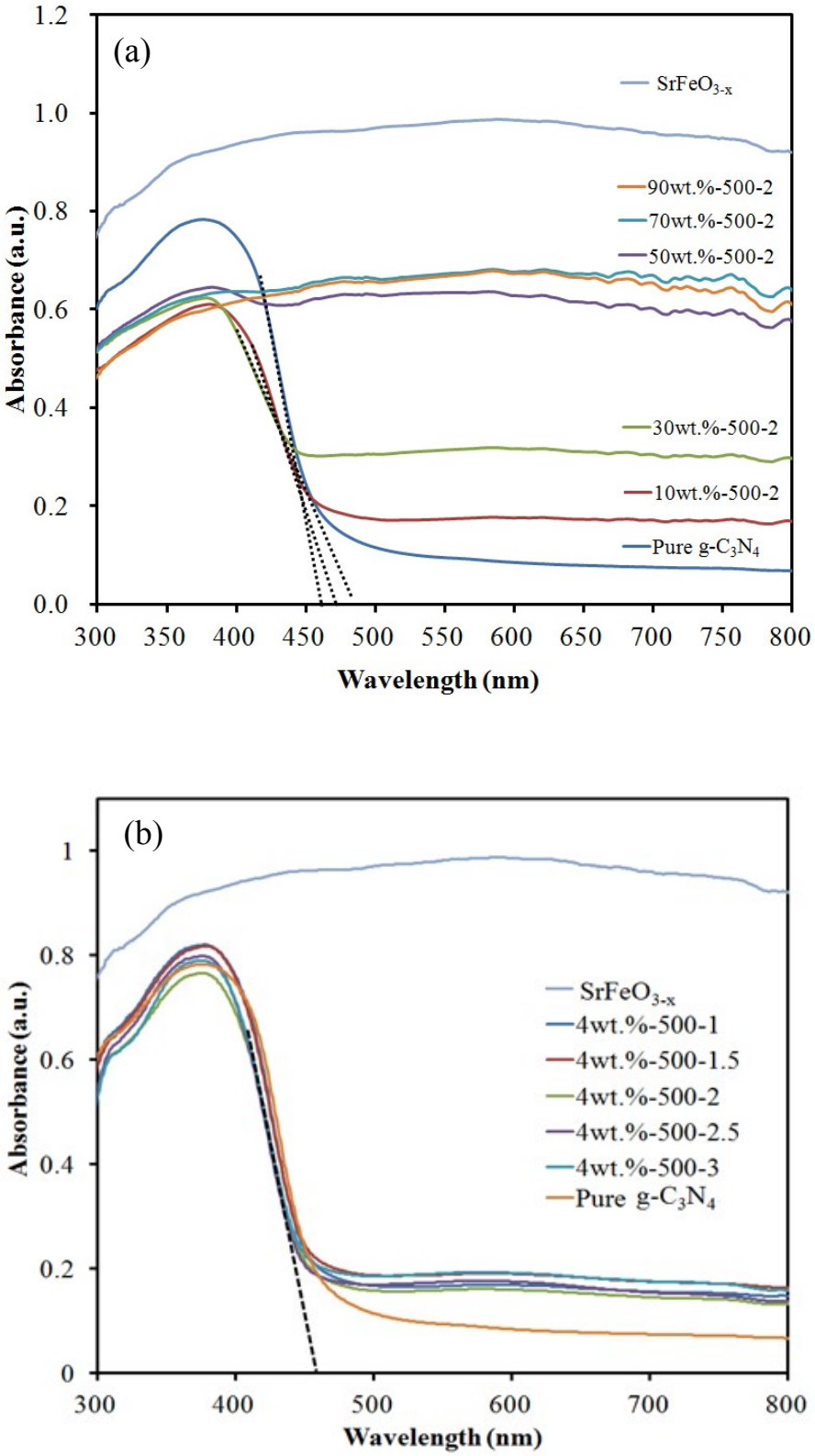

Figure S10. UV-vis diffuse reflectance spectra of the $SrFeO_{3-x}/g\text{-}C_3N_4$ samples: (a) weight percentage and (b) reaction time.

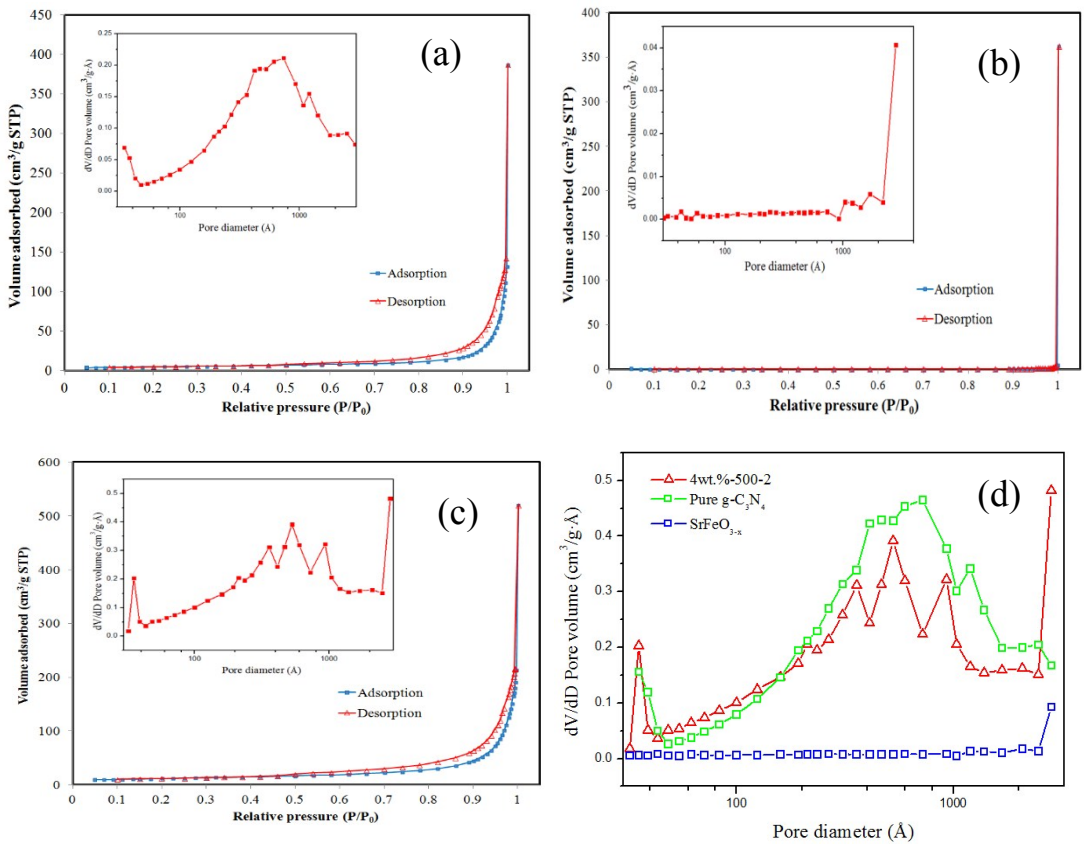

Figure S11. N_2 adsorption-desorption isotherm distribution curves and the pore distribution curves for (a) g-C_3N_4, (b) $SrFeO_{3-x}$, (c) $SrFeO_{3-x}$/g-C_3N_4 , and (d) xxxxx.

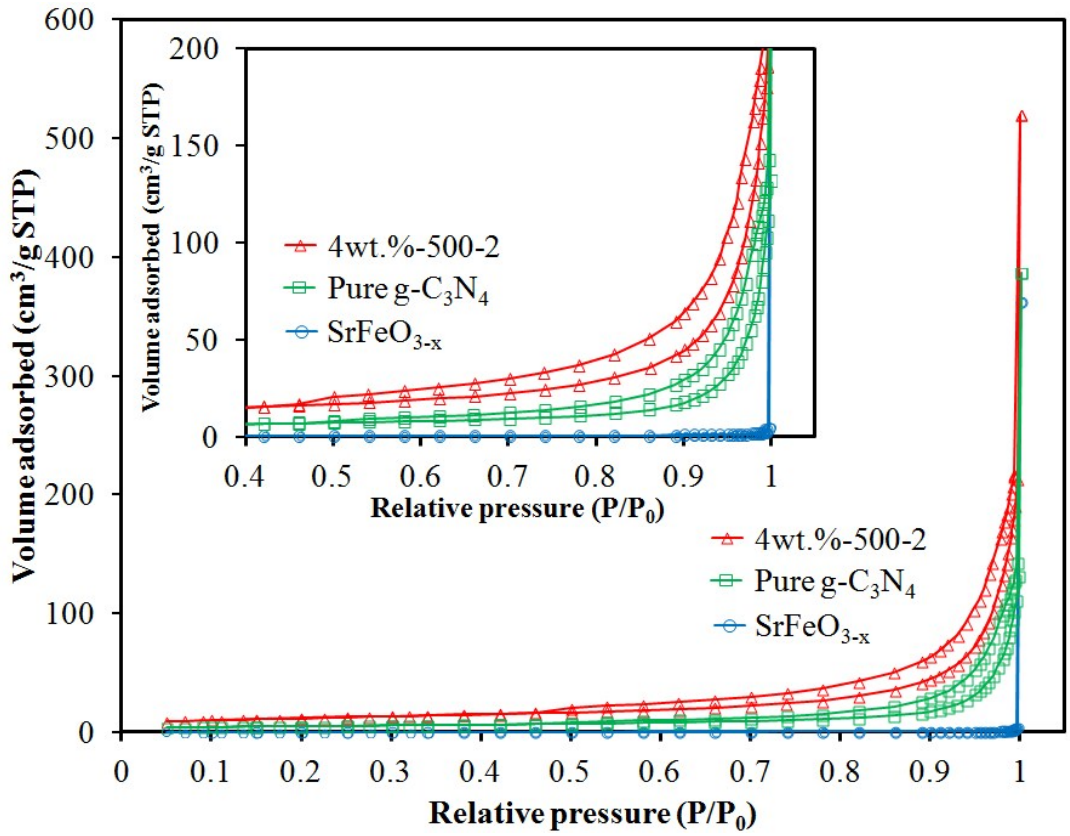

Figure S12. N_2 adsorption–desorption isotherm distribution curves for as-prepared $SrFeO_{3-x}$/g-C_3N_4, $SrFeO_{3-x}$, and g-C_3N_4 samples (inset: enlarged view).

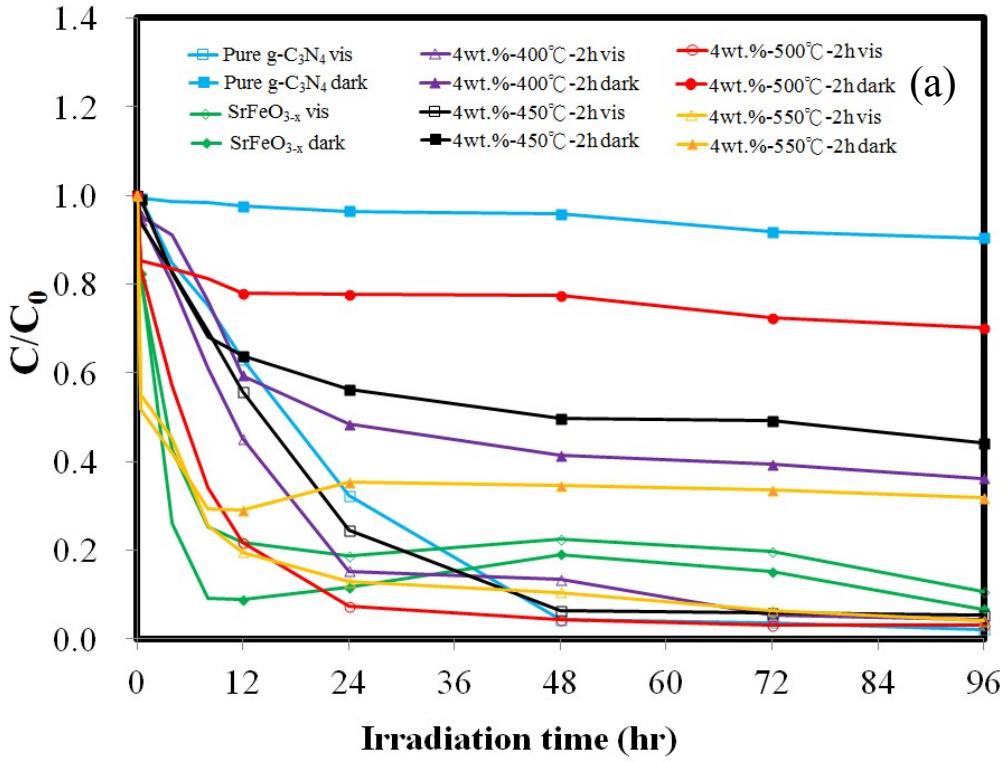

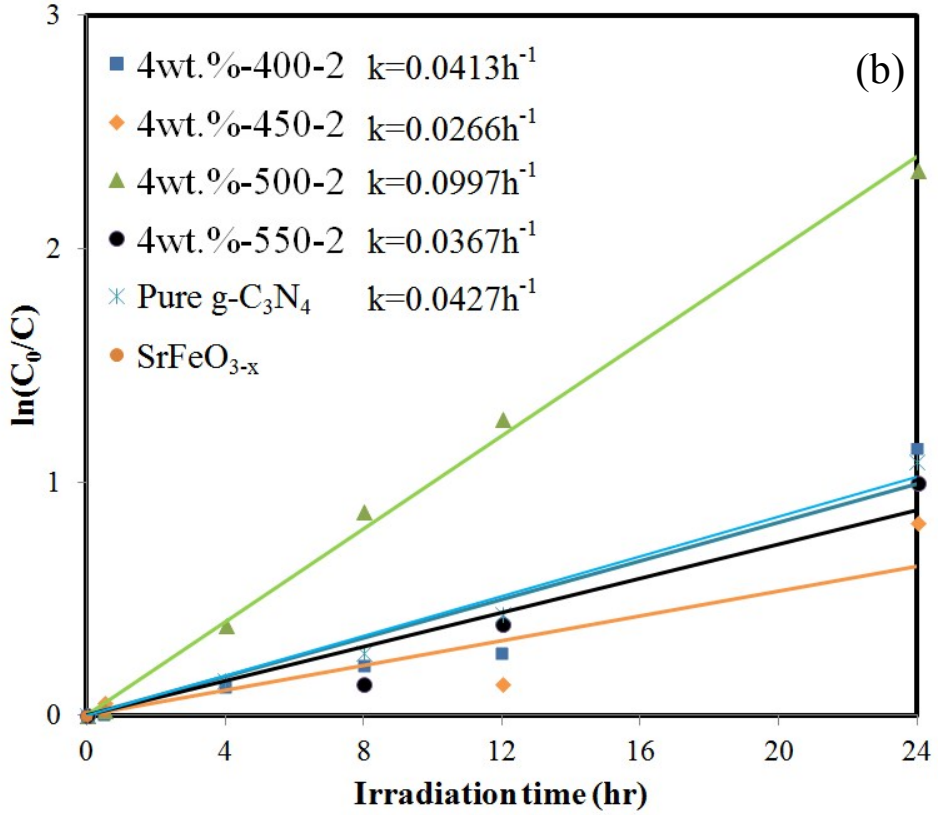

Figure S13. Photocatalytic degradation of CAP as a function of irradiation time over 4wt.% $SrFeO_{3-x}$/g-C_3N_4 photocatalysts. (Sintering conditions: temp = 400-550°C, time = 2 h)

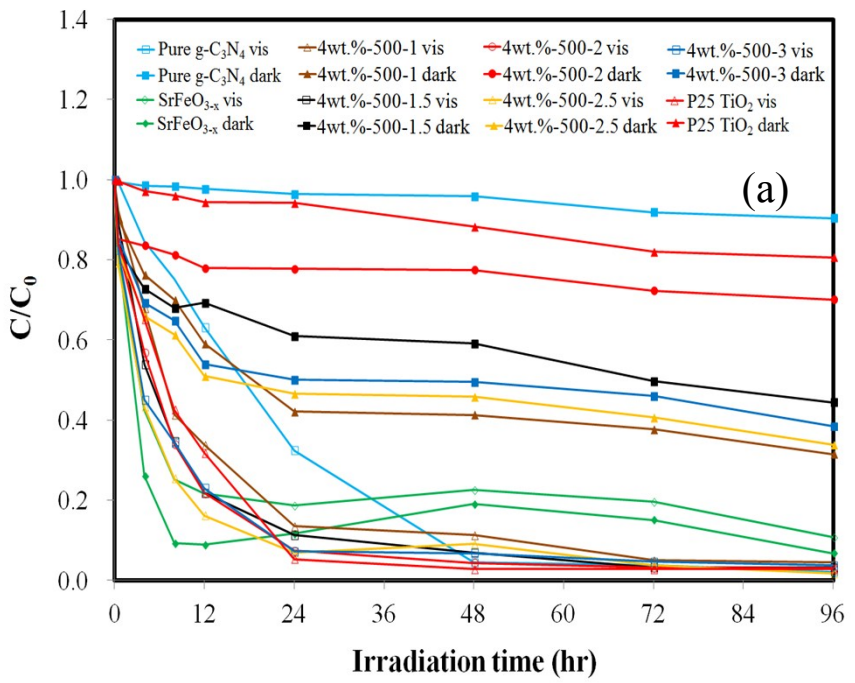

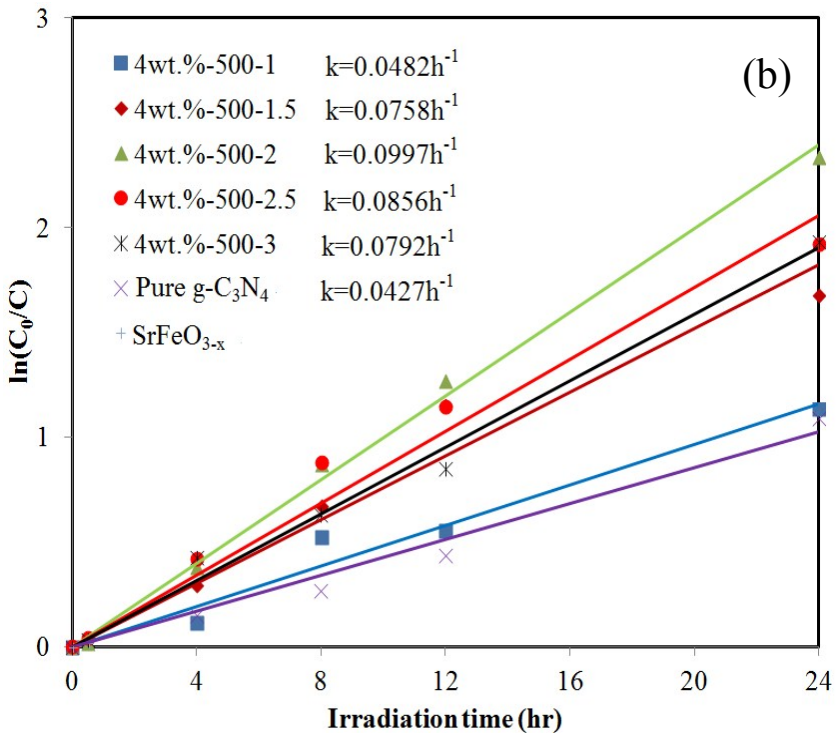

Figure S14. Photocatalytic degradation of CAP as a function of irradiation time over 4wt.% $SrFeO_{3-x}$/g-C_3N_4 photocatalysts. (Sintering conditions: temp = 500°C, time = 1-3 h)

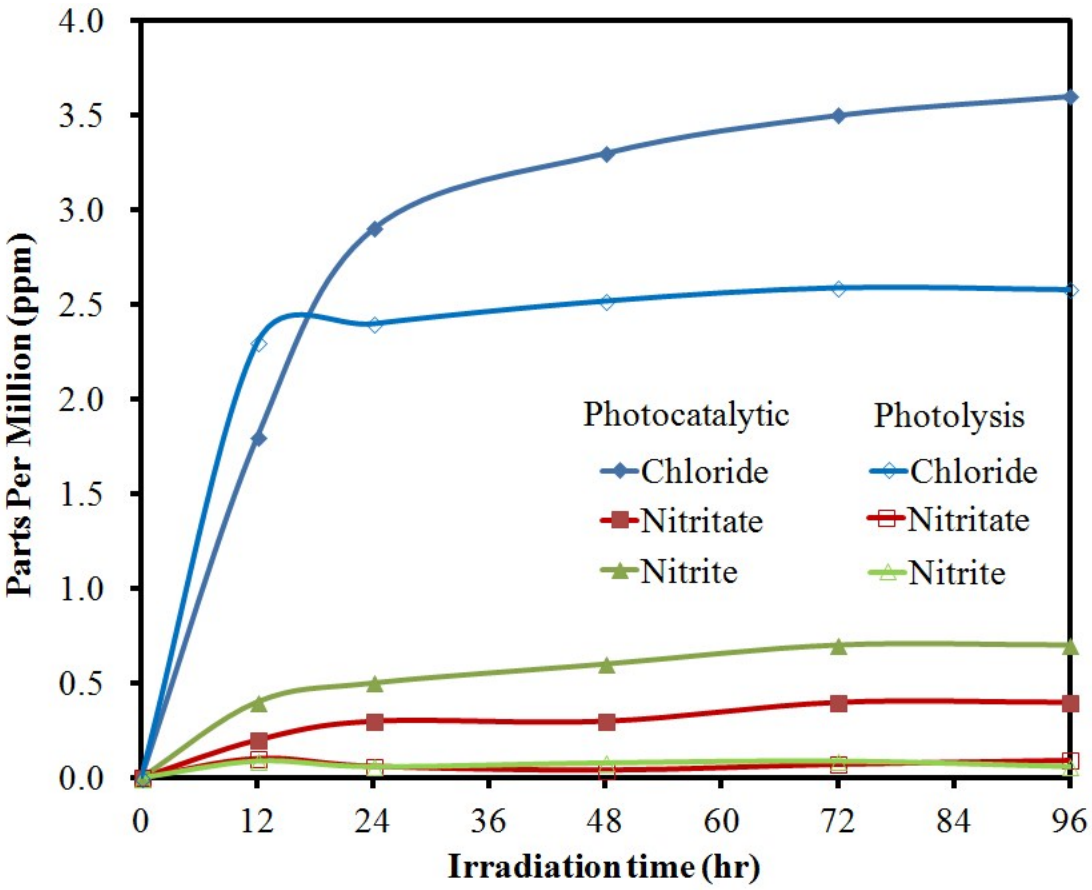

Figure S15. Temporal concentration of Cl^-, NO_3^-, and NO_2^- ions changes during the photocatalytic degradation and photolysis of CAP over aqueous 4wt.% $SrFeO_{3-x}$/g-C_3N_4 under visible light irradiation.

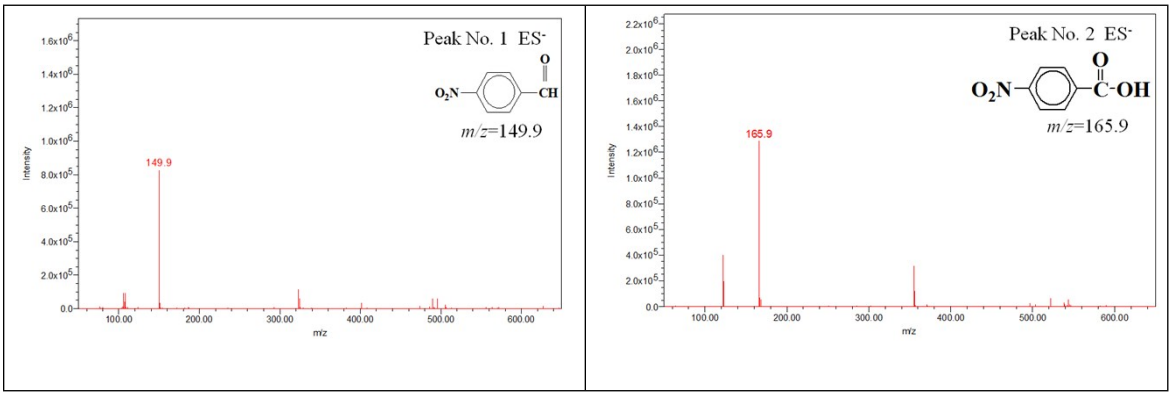

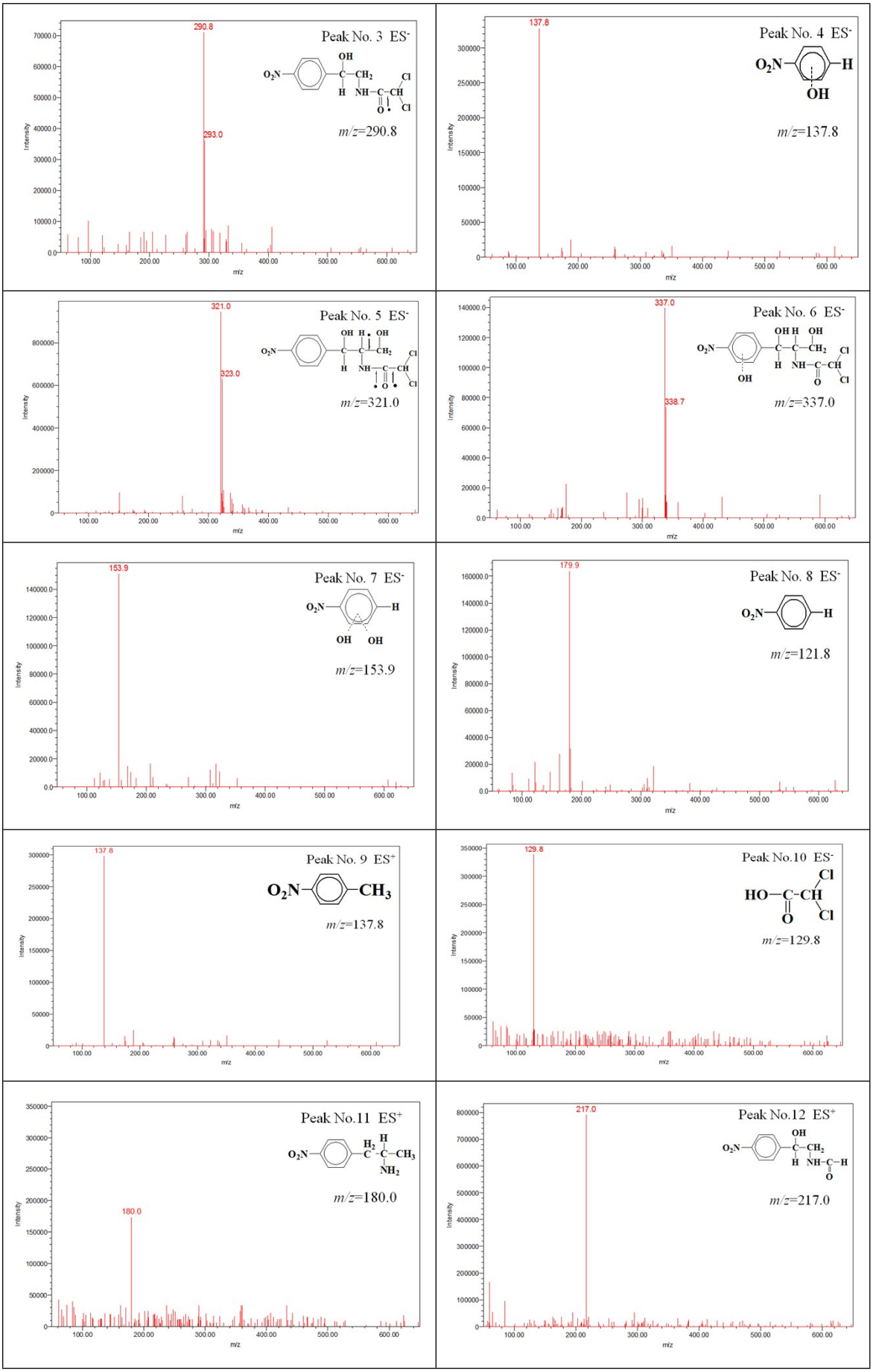
Peak No. 3 ES-
m/z=290.8
290.8
293.0
Peak No. 4 ES-
m/z=137.8
137.8
Peak No. 5 ES-
m/z=321.0
321.0
323.0
Peak No. 6 ES-
m/z=337.0
337.0
338.7
Peak No. 7 ES-
m/z=153.9
153.9
Peak No. 8 ES-
m/z=121.8
179.9
Peak No. 9 ES+
m/z=137.8
137.8
Peak No.10 ES-
m/z=129.8
129.8
Peak No.11 ES+
m/z=180.0
180.0
Peak No.12 ES+
m/z=217.0
217.0
Intensity
m/z

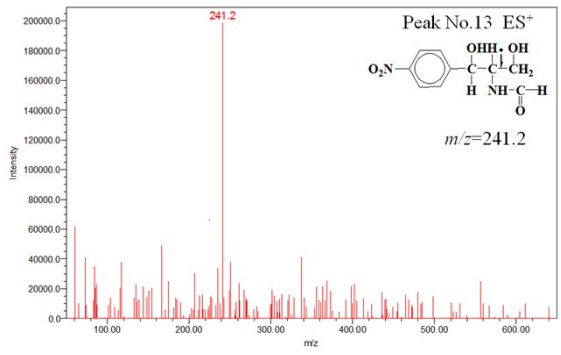

Figure S16. ESI mass spectra of the intermediates formed during the photodegradation of the CAP after they were separated by HPLC method.